

Herpes Simplex Virus Type 1 Infection Induces Activation and Recruitment of Protein Kinase C to the Nuclear Membrane and Increased Phosphorylation of Lamin B

Richard Park and Joel D. Baines*

Department of Microbiology and Immunology, Cornell University, Ithaca, New York 14853

Received 11 May 2005/Accepted 4 October 2005

We report that herpes simplex virus type 1 (HSV-1) infection leads to the recruitment of protein kinase C (PKC) to the nuclear rim. In HEP-2 cells, PKC recruitment to the nuclear rim was initiated between 8 h and 12 h postinfection. PKC δ , a proapoptotic kinase, was completely recruited to the nuclear rim upon infection with HSV-1. PKC α was less dramatically relocalized mostly at the nuclear rim upon infection, although some PKC α remained in the cytoplasm. PKC ζ -specific immunofluorescence was not significantly relocated to the nuclear rim. The U_L34 and U_L31 proteins, as well as their association, were each required for PKC recruitment to the nuclear rim. The HSV-1 U_S3 protein product, a kinase which regulates the phosphorylation state and localization of U_L34, was not required for PKC recruitment to the nuclear rim; however, it was required for proper localization along the nuclear rim, as PKC appeared unevenly distributed along the nuclear rim of cells infected with U_S3 null and kinase-dead mutants. HSV-1 infection induced the phosphorylation of both lamin B and PKC. Elevated lamin B phosphorylation in HSV-1-infected cells was partially reduced by inhibitors of PKC. The data suggest a model in which kinases that normally disassemble the nuclear lamina during apoptosis are recruited to the nuclear membrane through functions requiring U_L31 and U_L34. We hypothesize that the recruitment of PKC functions to phosphorylate lamin B to help modify the nuclear lamina and promote budding of nucleocapsids at the inner nuclear membrane.

The nuclear lamina is a filamentous protein meshwork lining the nucleoplasmic face of the inner nuclear membrane (INM) that confers structural support to the nucleus, provides chromatin anchoring sites, and may regulate higher-order chromatin structure and gene expression (14). The lamina is composed primarily of type V intermediate filament proteins called lamins, which have been grouped into two biochemically and functionally distinct categories: A-type and B-type. Like all intermediate filaments, lamins share a tripartite organization consisting of a conserved central α -helical rod domain flanked by N- and C-terminal non- α -helical head and tail domains of variable size and sequence (35). It is understood that individual lamins will dimerize and intertwine via their rod domains and associate in a head-to-tail fashion via the terminal domains, giving rise to rigid filaments that comprise the lamina meshwork.

Despite its relative insolubility and structural rigidity, the lamina is a dynamic structure whose disassembly during mitosis is regulated primarily by phosphorylation of the lamins at conserved serine residues flanking the α -helical rod domain (15, 35). During apoptosis, one step in the irreversible disassembly of the nuclear lamina (26, 36) involves hyperphosphorylation of lamin B proteins by protein kinase C δ (PKC δ) (4). Distinct from mitotic lamin phosphorylation, major PKC phosphorylation sites on lamin proteins have been mapped to serine residues located in close proximity to the nuclear localization signal in the C-terminal tail domain (16). Other cellular lamin kinases include mitogen-associated protein kinases and cyclic AMP-dependent protein kinase.

The PKC family consists of 12 structurally related serine-threonine kinases which function in a variety of cellular processes, including differentiation, proliferation, apoptosis, and carcinogenesis. PKCs have been grouped into three structurally and functionally distinct subfamilies: conventional PKCs, novel PKCs, and atypical PKCs. The activation of conventional PKCs requires diacylglycerol, Ca²⁺, and phosphatidylserine (PS). Activation of novel PKCs requires diacylglycerol and PS but not Ca²⁺, whereas atypical PKCs respond only to PS. The activation of conventional PKCs and novel PKCs also involves recruitment to cellular membranes, whereas atypical PKC activation does not (4, 25). All PKC family members are also regulated by phosphorylation, specifically at a conserved threonine residue within a motif (TFCGT) located within their activation domains. This PKC phosphorylation serves to regulate PKC activity and is catalyzed by phosphoinositide-dependent kinase 1, which is itself recruited to membranes by PtdIns(3,4,5)P₃. The phosphoinositide-dependent kinase 1-dependent activation loop phosphorylation occurs in conjunction with C-terminal phosphorylations which lock the kinase domains in their active conformations. In the nonphosphorylated form, PKC catalytic activity is virtually undetectable; however, in the membrane-bound, activated, and phosphorylated state, substrate phosphorylation is efficient (24). During apoptosis, PKC δ , a novel PKC, has been shown to translocate to the nuclear membrane and to phosphorylate lamin B at the C-terminal domain, thereby inducing apoptotic lamina disassembly (4, 6, 9, 10). PKC β II has also been shown to phosphorylate and thereby solubilize lamin B (8). Conversely, PKC α has been shown to bind lamin A protein yet functions as an apoptosis inhibitor (9, 20).

* Corresponding author. Mailing address: Department of Microbiology and Immunology, Cornell University, Ithaca, NY 14853. Phone: (607) 253-3391. Fax: (607) 253-3384. E-mail: jdb11@cornell.edu.

Herpes simplex virus type 1 (HSV-1), like all members of the herpesvirus family, assembles progeny nucleocapsids within the host cell nucleus. Fully formed DNA-containing nucleocapsids must then exit the nucleus by budding through the INM and outer nuclear membrane (ONM) in a well-documented envelopment-deenvelopment process (21). As the insoluble nuclear lamina would present a significant barrier to capsid envelopment at the INM, it is logical that herpesviruses would devise or adopt means of modifying the nuclear lamina to promote nucleocapsid egress. For HSV-1, the viral proteins U_L34 and U_L31 have been implicated in nuclear egress (7, 30). Studies have shown that the U_L34 and U_L31 proteins (pU_L34 and pU_L31 , respectively) associate to form a complex which localizes to the nuclear rim of the infected cell (3, 28, 29). Although the U_L34 - U_L31 complex has been shown to induce structural alterations of the nuclear lamina (27, 34), the mechanism by which this complex facilitates HSV-1 nucleocapsid egress has not yet been defined.

Proper localization of the U_L31 - U_L34 complex is dependent upon the kinase activity of the HSV-1 U_S3 protein. In the absence of U_S3 kinase activity, the U_L31 and U_L34 proteins colocalize in punctate extensions of the nuclear membrane (31). Although U_L34 is clearly a substrate of the U_S3 kinase, mutational analysis has shown that a substrate(s) other than U_L34 is necessary to explain the mechanism by which U_S3 modulates the localization of the U_L31 - U_L34 complex in the NM (31).

Increasing evidence indicates that the HSV-1 U_L34 - U_L31 -mediated mechanism of nucleocapsid egress may be conserved, or at least share significant similarities, among the various members of the herpesvirus family. Homologs of U_L34 and U_L31 have been identified in HSV-2, pseudorabies virus, murine cytomegalovirus (MCMV; M50 and M53), and Epstein-Barr virus (BFRF1 and BFLF2) (12, 13, 21, 23). Furthermore, these various U_L34 - U_L31 homologous pairs share a number of characteristics: (i) they are codependent for proper targeting to the nuclear rim; (ii) they facilitate nuclear egress of their respective nucleocapsids; and (iii) they share the capacity to interact with, and to induce structural alterations to, the nuclear lamina. Muranyi et al. (23) demonstrated that M50 and M53 recruit cellular PKC to the nuclear lamina and showed that this recruitment was concomitant with a phosphorylation of lamins A/C and B (23). They postulated that M50 and M53 facilitate nucleocapsid egress by recruiting PKC to the INM to phosphorylate lamins. This lamin phosphorylation was proposed to then mediate a partial dismantling of the nuclear lamina to allow viral capsids to traverse the lamina and dock at the INM.

In consideration that MCMV infection leads to a recruitment of PKC to the nuclear lamina and a phosphorylation of lamin proteins, we investigated whether HSV-1 infection also induces a recruitment of PKC to the nuclear lamina.

MATERIALS AND METHODS

Cells and viruses. HEP-2 cells, Vero cells, and HeLa cells were maintained in Dulbecco's modified Eagle's medium supplemented with 10% newborn calf serum, penicillin, and streptomycin. The construction and maintenance of the U_L34 -expressing cell line, R1310, and the U_L31 -expressing cell line, clone 7, were described previously (18, 19).

The wild-type HSV-1 (F) was described previously (11). The construction and growth characteristics of the U_L34 -null mutant, vRR1072, the U_L31 -null mutant, v3161, the U_L34 - U_L31 association-defective mutant, v3480, the U_S3 -null mutant,

R7037, and the U_S3 kinase-defective mutant, vRR1204#1 (K220A) were also described previously (19, 20, 30, 31).

Antibodies and PKC inhibitors. All anti-PKC and anti-lamin B antibodies were obtained from Santa Cruz Biotechnology, Inc. Anti-ICP4 antibody was obtained from the Rumbaugh-Goodwin Institute for Cancer Research. Fluorescein isothiocyanate (FITC)-conjugated anti-goat and Texas Red-conjugated anti-rabbit secondary antibodies were obtained from Santa Cruz Biotechnology, Inc., and Cy5-conjugated anti-mouse secondary antibody was obtained from Jackson ImmunoResearch Inc. The PKC inhibitors rottlerin and RO-31-7549 were purchased from Santa Cruz Biotechnology, Inc.

Indirect immunofluorescence assay and confocal microscopy. HEP-2 cells and HeLa cells were seeded on glass coverslips in six-well plates at 80% confluence and grown overnight at 37°C. Cells were either mock infected or infected with wild-type (F) or U_S3 mutant strains of HSV-1 at a multiplicity of infection (MOI) of 5 to 10. In the case of the U_L34 and U_L31 mutant strains, cells were infected at an MOI of 0.3 to 0.5, reflecting lower viral stock titers. At 2, 4, 8, 12, or 16 h postinfection, cells were washed three times with phosphate-buffered saline (PBS) and fixed with methanol at -20°C for 20 min. Cells were washed again with PBS and then incubated for 45 min at room temperature in blocking solution (PBS containing 10% filtered human serum). Cells were then probed with primary antibodies specific for lamin B, PKC, and HSV-1 ICP4 for 1 h. Cells were washed with PBS and blocked again for 15 min. Cells were then incubated at room temperature with FITC-, Texas Red-, and Cy5-conjugated secondary antibodies for 1 h. Coverslips were washed with PBS, rinsed in distilled H₂O, and mounted using Vectashield mounting medium (Vector Laboratories, United Kingdom). Slides were analyzed with a confocal laser scanning microscope equipped with krypton, argon, and helium-neon lasers under a 63× oil immersion objective and a 10× ocular objective in light filtered to wavelengths appropriate for excitation of FITC, Texas Red, and Cy5 fluorochromes or in transmitted light. Images were analyzed by Nomarski differential interference contrast imaging, and digital images were acquired with Fluoview version 2.1.39 software. There was minimal emission of more than one fluorochrome at a given excitation wavelength.

Immunoprecipitation and kinase assay. Confluent cultures of HEP-2 cells were mock or HSV-1 (F) infected at an MOI of 5. At 13 h postinfection, cells were washed three times with methionine-free, phosphate-free minimum essential Eagle's medium (Gibco BRL) and then incubated with the same medium containing 5% dialyzed fetal bovine serum and 100 μ Ci of [³²P]orthophosphate (Amersham). PKC-specific inhibitors dissolved in dimethyl sulfoxide were also added at this point. At 16 h postinfection, cells were washed with PBS, harvested by cell scraper, and pelleted by centrifugation at 1,200 \times g. On ice, pellets were resuspended in RIPA buffer (25 mM Tris-Cl [pH 7.4], 1% NP-40, 0.5% Na-deoxycholate, 200 mM NaCl, 1 mM EDTA, 0.1% sodium dodecyl sulfate [SDS]) supplemented with 1 mM Na₃VO₄, 10 mM NaF, 1 μ g/ml aprotinin, 1 μ g/ml leupeptin, 1 μ g/ml pepstatin A, 1 mM phenylmethylsulfonyl fluoride, and Complete EDTA-free protease inhibitor cocktail (Roche) for 20 min. During this incubation, the lysate was aspirated several times through a 25-gauge needle. The lysate was then centrifuged at 12,000 \times g for 15 min at 4°C, and the pellet was discarded.

Lysate was then precleared by incubation with protein A/G-agarose beads at 4°C for 1 h. Beads were removed by pelleting at 1,200 \times g for 1 min at 4°C. Lysate was then incubated with anti-lamin B or anti-PKC antibodies overnight at 4°C. Protein A/G-agarose was added, and the lysate was incubated at 4°C for an additional 2 h. Precipitated proteins were pelleted at 1,200 \times g for 1 min at 4°C, washed three times with RIPA buffer at 4°C, and then resolved on a 10% SDS-polyacrylamide gel electrophoresis (SDS-PAGE) gel. The gel was dried and analyzed by autoradiography.

Immunoblot analysis. Confluent cultures of HEP-2 cells were mock or HSV-1 (F) infected at an MOI of 5. At 16 h postinfection, cells were washed three times with PBS, removed into PBS, and pelleted at 1,200 \times g at 4°C. Pelleted cells were resuspended in 2 \times Laemmli buffer and briefly sonicated to facilitate loading of insoluble material. Samples were boiled for 5 min, resolved by SDS-PAGE on a 10% gel, and then electrically transferred onto a nitrocellulose membrane. The nitrocellulose was incubated for 1 h at room temperature in blocking solution: PBS containing 5% (wt/vol) nonfat milk and 0.1% Tween 20. The blot was then incubated with anti-lamin B or anti-PKC antibody overnight at 4°C, washed with PBS-Tween, and then incubated with horseradish peroxidase (HRP)-conjugated secondary antibody for 2 h at room temperature. The blot was washed again, and the labeled proteins were visualized using an ECL (Amersham) chemiluminescence kit according to the manufacturer's instructions.

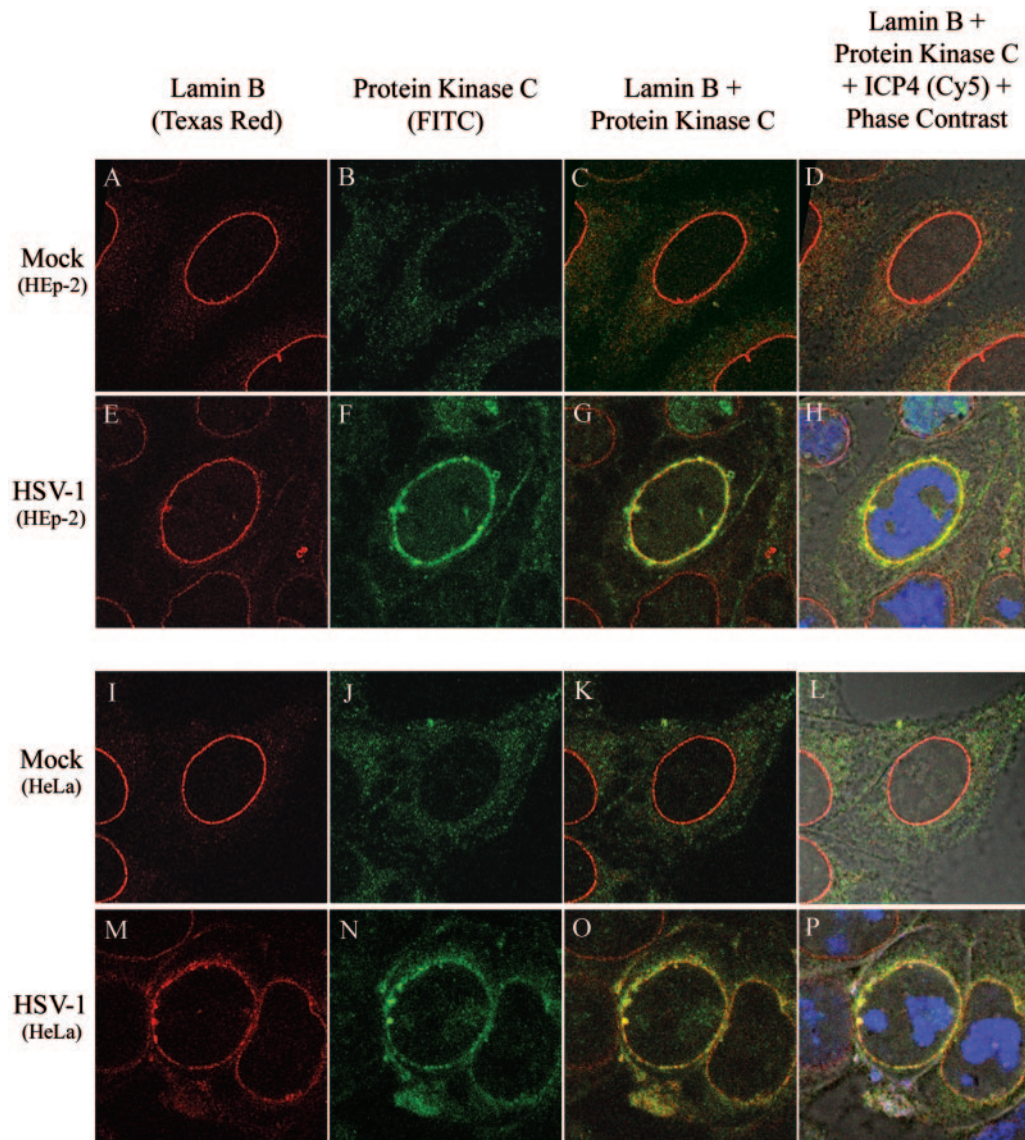


FIG. 1. Digital images of confocal fluorescence micrographs of mock-infected (A to D and I to L) and HSV-1 (F)-infected (E to H and M to P) HEP-2 cells (A to H) and HeLa cells (I to P). Cells were fixed in methanol at 16 h postinfection and incubated with anti-PKC, anti-lamin B, and anti-ICP4 antibody. Anti-PKC antibody was stained with FITC-conjugated secondary antibody (green channel), anti-lamin B antibody was stained with Texas Red-conjugated secondary antibody (red channel), and ICP4 was stained with Cy5-conjugated secondary antibody (blue channel).

RESULTS

Cellular protein kinase C is recruited to the nuclear lamina during HSV-1 infection in two human cell lines. To determine whether protein kinase C was recruited to the nuclear membrane, confluent monolayers of HEP-2 and HeLa cells were either mock infected or infected with wild-type HSV-1 (F) and then fixed with -20°C methanol at 16 h postinfection. Fixed cells were costained with three antibodies: (i) a rabbit polyclonal antiserum which recognizes all PKC family members (sc-10800; Santa Cruz Biotechnology), (ii) a goat polyclonal antiserum specific for lamin B protein (sc-6216; Santa Cruz Biotechnology), and (iii) a mouse monoclonal antibody specific for the HSV-1 ICP4 protein (no. 1101; Rumbaugh Goodwin Institute). Bound anti-lamin

B, anti-PKC, and anti-ICP4 antibodies were visualized with Texas Red-conjugated bovine anti-goat, FITC-conjugated bovine anti-rabbit, and Cy5-conjugated donkey anti-mouse secondary antibodies, respectively. Digital images were acquired by confocal microscopy, and representative examples are shown in Fig. 1.

Immunostained mock-infected HEP-2 and HeLa cells (Fig. 1A to D and I to L) contained smooth oval lamin B staining that was uniformly and tightly distributed around the nuclear rim. PKC-specific staining in both mock-infected HEP-2 and HeLa cells was faintly and diffusely detected throughout the cytoplasm in a grainy or speckled pattern and was localized in the cytoplasm. No PKC-specific staining was detectable in the nucleus or along the nuclear rim.

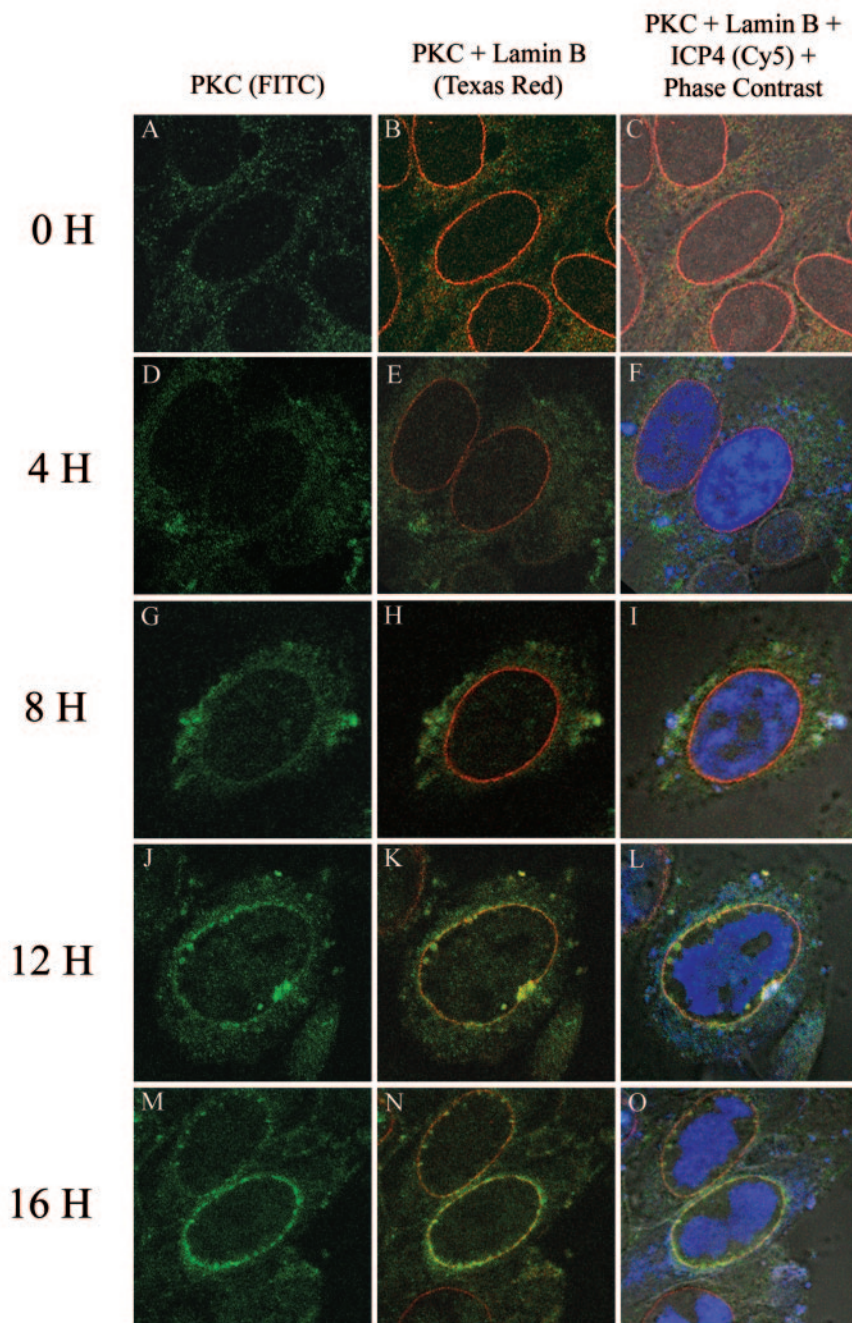


FIG. 2. Time course of PKC upregulation and recruitment to the nuclear rim. Digital images of confocal fluorescence micrographs were taken of HEp-2 cells infected with HSV-1 (F). At 0 h (A to C), 4 h (D to F), 8 h (G to I), 12 h (J to L), and 16 h (M to O) postinfection, cells were fixed and stained for PKC (FITC; green channel), lamin B (Texas Red; red channel), and ICP4 (Cy5; blue channel).

In contrast to the smooth oval uniform staining seen in mock-infected cells, lamin B-specific immunostaining of HEp-2 and HeLa cells infected 16 h previously with HSV-1 (F) (Fig. 1E to H and M to P) contained morphological alterations, including invaginations or concavities of the nuclear rim. Moreover, the staining was not uniform along the nuclear rim but instead contained areas of thickened or denser lamin B staining and areas of thinner or lighter staining. HSV-1-induced lamin B aggregates were also pronounced in cytoplasmic regions immediately adjacent to the

abnormally concave portions of nuclear lamina in infected HeLa cells and closely resembled the cytoplasmic accumulations of lamin B receptor (LBR) reported by Scott and O'Hare in HSV-1-infected COS-1 cells (32). We therefore conclude that HSV-1 (F) infection of both HEp-2 and HeLa cells at 16 h postinfection resulted in morphological distortions to the nuclear lamina as indicated by lamin B staining.

In contrast to the diffuse, low-level PKC expression localized within the cytoplasm of mock-infected cells, most HSV-1-in-

ected cells showed an increased level of PKC immunostaining. The elevated PKC immunostaining localized primarily at the nuclear rim, although minor amounts were detectable in the cytoplasm and in association with the plasma membrane. As seen by the yellowish staining of the combined images (Fig. 1H and P), the elevated PKC immunostaining extensively colocalized with lamin B at the nuclear rim and within cytoplasmic regions immediately adjacent to invaginations or concave portions of the nuclear membrane. These data therefore indicate that infection with HSV-1 (F) induces an upregulation of PKC expression and a clear recruitment of PKC to the nuclear rim.

Time course of PKC recruitment in HSV-1-infected HEP-2 cells. To determine when PKC was recruited during the course of infection, HEP-2 cells were fixed and stained for PKC and lamin B at different times postinfection (Fig. 2). At 0 h postinfection (Fig. 2A to C), the lamin B and PKC staining resembled a mock infection as described above. At 4 h postinfection (Fig. 2D to F), the morphology of the nuclear lamina appeared unchanged, and PKC expression remained diffusely localized throughout the cytoplasm. ICP4-specific staining was localized in both the nucleus and cytoplasm of infected cells, whereas at later times it localized in the nucleus, as previously described (17). At 8 h postinfection (Fig. 2G to I), some distortions to the otherwise-smooth-appearing nuclear lamina were apparent. Also at 8 h postinfection, a faint yet discernible increase of PKC-specific staining was visible at the nuclear rim. By 12 h postinfection (Fig. 2J to L), morphological distortions to the nuclear lamina closely resembled those seen at 16 h postinfection and shown in Fig. 1. Also at 12 h postinfection, a clear recruitment of PKC to the nuclear rim was seen. PKC recruitment to the nuclear rim, however, appeared incomplete, since PKC was distributed unevenly at the nuclear rim compared to later times postinfection. The phase-contrast images at 12 h and 16 h postinfection indicate that the recruitment of PKC to the nuclear rim was not a consequence of cell shrinkage that might cause cytoplasmic contents to concentrate around the nuclear rim. We conclude that, at least in HEP-2 cells, PKC is recruited to the nuclear rim beginning at 8 h p.i. This would suggest PKC recruitment coincides with late viral gene expression.

Specific PKC isoforms are recruited to the nuclear lamina during HSV-1 infection. The immunofluorescence assay (IFA) experiments described above and elsewhere in this study were designed to characterize changes in localization of any and all PKC enzymes inasmuch as the studies employed a commercial antibody with reported broad reactivity with all PKC family members of mouse, rat, and human, *Drosophila*, and *Xenopus* origins (sc-10800 data sheet; Santa Cruz Biotechnology). To investigate whether the observed PKC recruitment to the nuclear lamina involves specific PKC subgroups or isoforms, three antibodies which recognize a single specific PKC isoform from each of the three PKC subgroups (conventional PKCs, novel PKCs, and atypical PKCs) were used. These included antibodies specific for PKC α , a conventional PKC (sc-208; Santa Cruz Biotechnology) (Fig. 3A to D), PKC δ , a novel PKC (sc-937; Santa Cruz Biotechnology) (Fig. 3E to H), and PKC ζ , an atypical PKC (sc-216; Santa Cruz Biotechnology) (Fig. 3I to L).

In mock-infected HEP-2 cells, PKC α localized at the plasma membrane and diffusely throughout the cytoplasm. There was virtually no PKC α detected along the nuclear rim or within the nucleoplasm and no detectable colocalization with lamin B

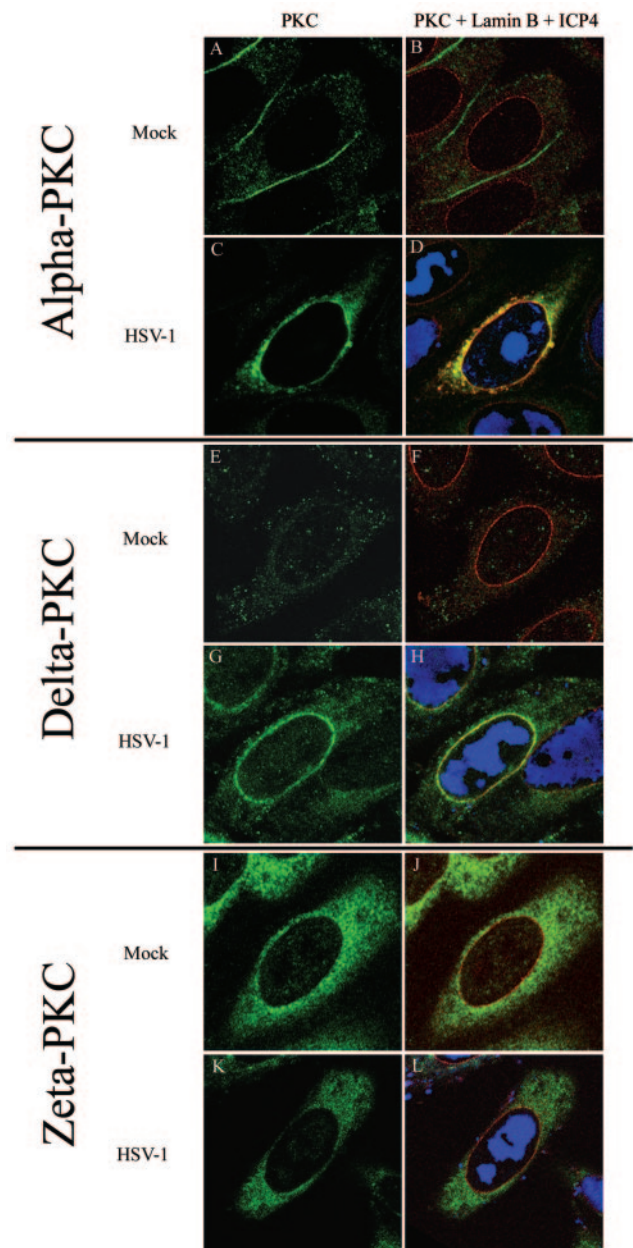


FIG. 3. Digital confocal images of mock-infected or HSV-1 (F)-infected HEP-2 cells immunostained with PKC-specific antibodies. At 16 h postinfection, cells were fixed with methanol and incubated with anti-lamin B antibody, anti-ICP4 antibody, and one of the following PKC-specific antibodies: anti-PKC α (A to D), anti-PKC δ (E to H), anti-PKC ζ (I to L). Anti-PKC antibodies were stained with FITC-conjugated secondary antibody (green channel), anti-lamin B antibody was stained with Texas Red-conjugated secondary antibody (red channel), and ICP4 was stained with Cy5-conjugated secondary antibody (blue channel).

(Fig. 3B). In contrast, in HSV-1-infected cells at 16 h postinfection, clear recruitment of PKC α to the nuclear rim and colocalization with lamin B staining was observed. However, the degree of PKC α recruitment varied from a tight association with the nuclear rim seen in a number of cells to a more loose association in which significant quantities of PKC α were

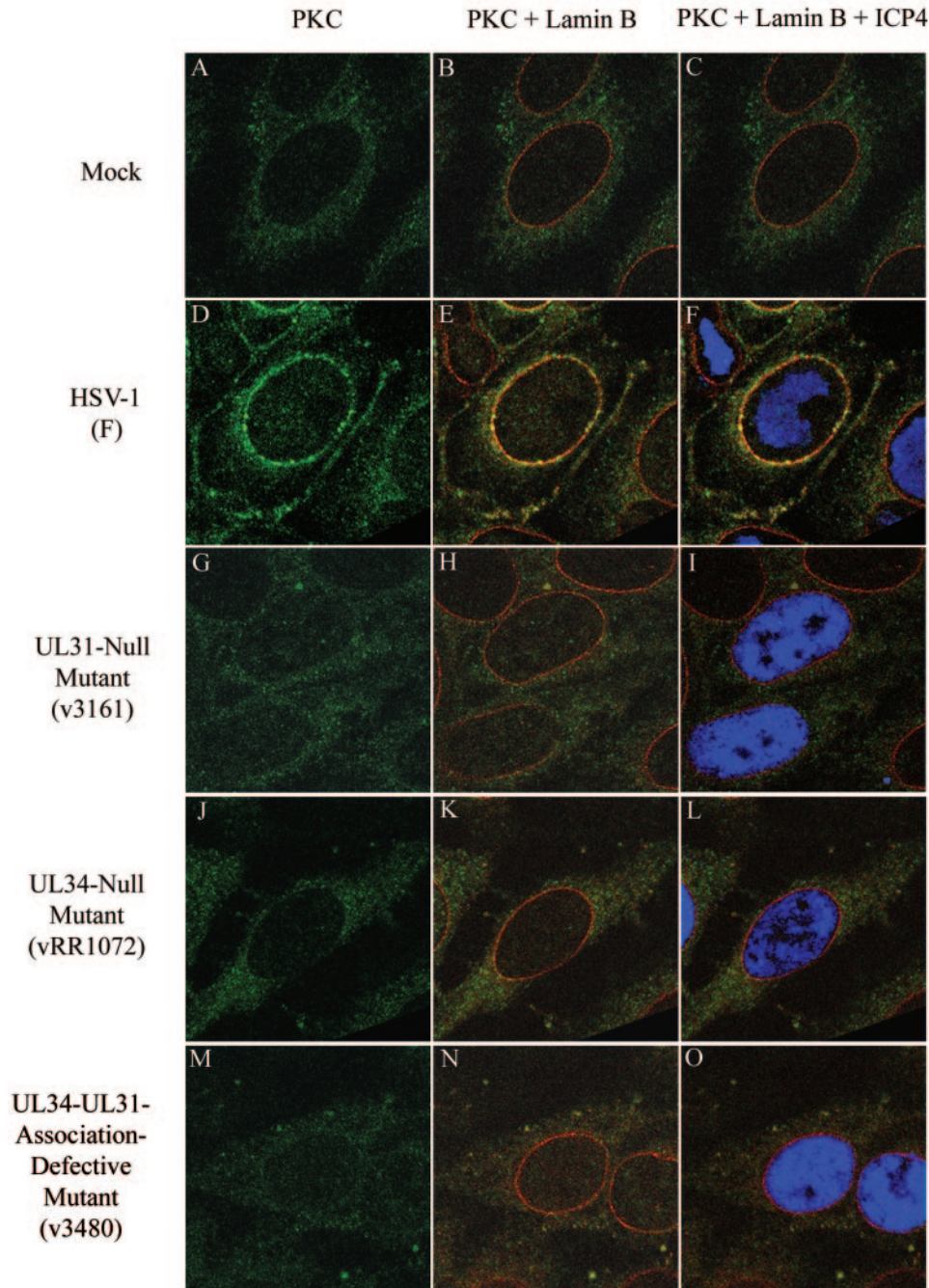


FIG. 4. Effects of U_L31 and U_L34 and their association on HSV-1-induced PKC recruitment. Digital confocal images show mock-infected HEp-2 cells (A to C) or HEp-2 cells infected with HSV-1 (F) (D to F), v3161 U_L31 -null HSV-1 mutant (G to I), vRR1072 U_L34 -null HSV-1 mutant (J to L), or v3480 U_L34 - U_L31 association-defective mutant (M to O). At 16 h postinfection, cells were fixed and stained for PKC (FITC; green channel), lamin B (Texas Red; red channel), and ICP4 (Cy5; blue channel).

localized to cytoplasmic perinuclear regions. PKC α thus appeared to undergo a partial recruitment to the nuclear rim in response to HSV-1 infection.

In mock-infected HEp-2 cells, PKC δ was barely detectable and localized diffusely throughout the cytoplasm. Unlike PKC α or PKC ζ staining, however, faint staining was also seen within the nuclei of mock-infected cells in a speckled pattern. In HSV-1-infected cells at 16 h postinfection, immunostaining

with PKC δ -specific antibody showed a significant increase in expression, a clearly defined recruitment to the nuclear rim, and colocalization with lamin B at the nuclear rim. Recruitment of PKC δ during HSV-1 infection appeared more robust and complete than that of the partial NM recruitment seen with PKC α .

PKC ζ staining in mock-infected cells exhibited a relatively high level of expression throughout the cytoplasm, with no

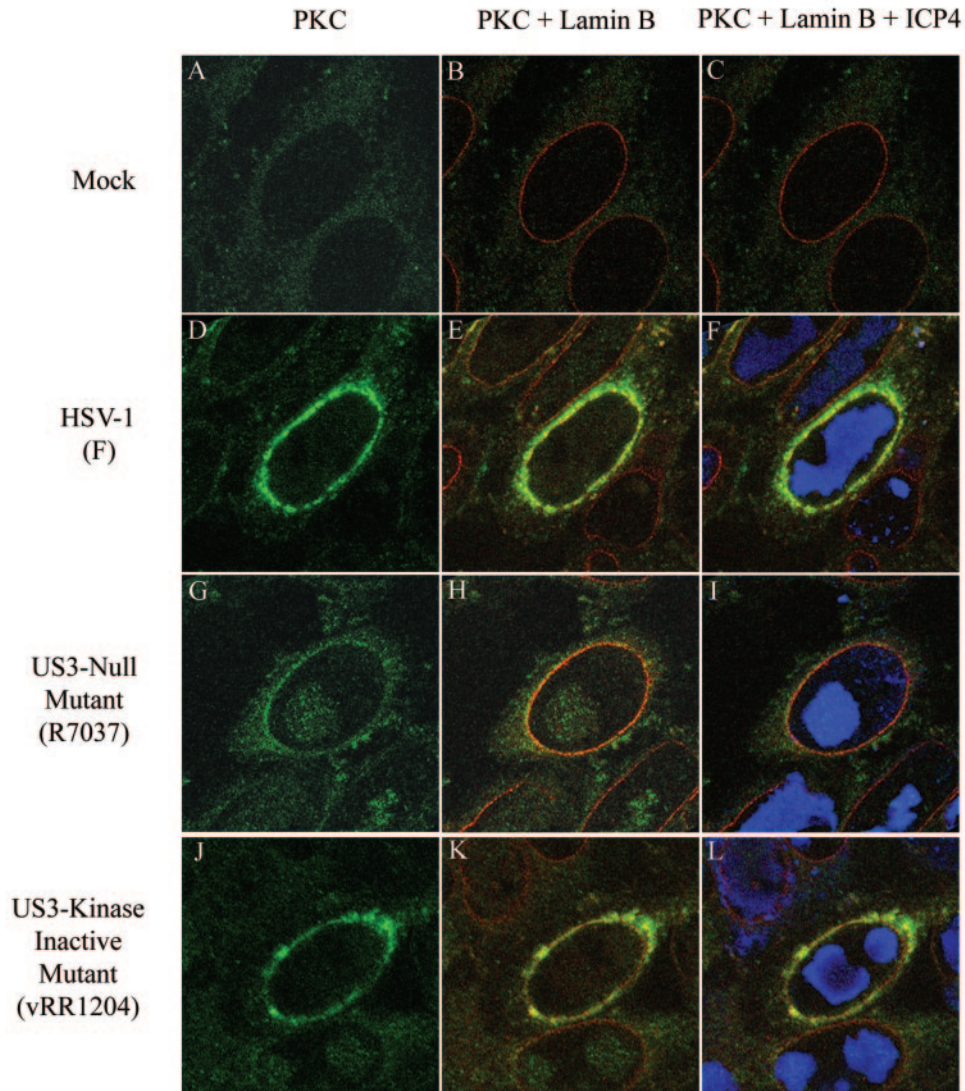


FIG. 5. Digital images of confocal fluorescence micrographs of mock-infected HEp-2 cells (A to C) or HEp-2 cells infected with HSV-1 (F) (D to F), R7037 U_{S3} -null HSV-1 mutant (G to I), or vRR1204 U_{S3} -kinase-defective HSV-1 mutant (J to L). At 16 h postinfection, cells were fixed and immunostained for PKC (FITC; green channel), lamin B (Texas Red; red channel), and ICP4 (Cy5; blue channel).

staining along the nuclear rim or within the nucleus and no colocalization with lamin B. In HSV-1-infected cells at 16 h postinfection, PKC ζ staining remained localized diffusely throughout the cytoplasm at levels that were slightly increased compared to those of mock-infected cells. In most infected cells, PKC ζ did not appear concentrated at the NM and did not colocalize with lamin B. However, in a subset of infected cells, PKC ζ staining was also seen at the nuclear rim in regions containing lamin B, as indicated by the yellowish staining in the combined image. Even within this subset of cells, however, much of the cytoplasmic PKC ζ remained evenly distributed throughout the cytoplasm at expression levels resembling those of mock-infected cells. PKC ζ therefore appeared to become recruited to the nuclear rim less reliably than did either PKC δ or PKC α .

HSV-1 U_{L31} and U_{L34} and their association are required for proper PKC recruitment. Muranyi et al. demonstrated that M50 and M53 are responsible for the recruitment of PKC to

the nuclear lamina of MCMV-infected cells (23). We therefore investigated whether the HSV-1 U_{L34} and U_{L31} proteins are also required for the observed recruitment of PKC to the nuclear rim during HSV-1 infection.

HEp-2 cells were mock infected or were infected with wild-type HSV-1 (F) or v3161, a U_{L31} deletion virus that produces no U_{L31} protein (19). Cells were fixed at 16 h postinfection, and PKC, lamin B, and ICP4 expression levels were observed by IFA. The pattern of PKC immunostaining in cells infected with the U_{L31} -null mutant (Fig. 4G to I) differed from that of mock-infected cells (Fig. 4A to C) and wild-type HSV-1 (F)-infected cells (Fig. 4D to F). In comparison with mock-infected cells, a faint yet detectable upregulation in PKC expression was evident in cells infected with the U_{L31} mutant virus; however, no distinct recruitment of PKC to the nuclear rim was observed. Thus, U_{L31} is required for the recruitment of PKC to the nuclear rim.

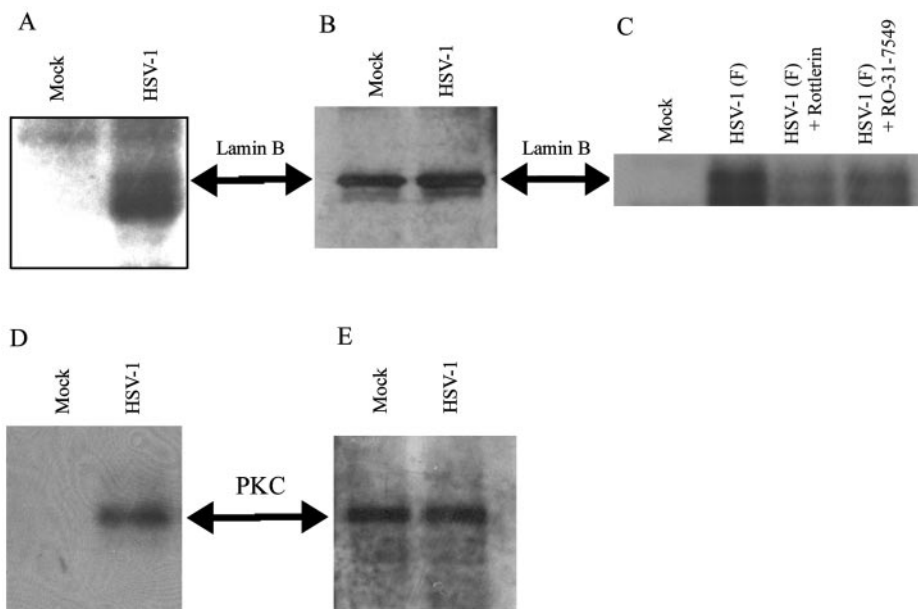


FIG. 6. Digital images of autoradiographs and immunoblots of immunoprecipitated lamin B and PKC labeled with [32 P]orthophosphate. HEp-2 cells were infected with HSV-1 (F), pulse-labeled with [32 P]orthophosphate, treated with PKC-specific inhibitors (C), lysed at 16 h postinfection, and immunoprecipitated with antibodies specific for lamin B (A and C) and PKC (D). Samples were electrophoretically resolved on an SDS denaturing polyacrylamide gel and processed for autoradiography. To confirm that lysates of mock-infected and HSV-1 (F)-infected cells contained nearly equal amounts of lamin B and PKC, immunoblots (B and E) of replicate crude lysates using antibodies against lamin B and PKC, respectively, were prepared according to standard protocols.

As mentioned above, U_L34 and U_L31 are codependent for their proper localization to the nuclear rim. To determine whether pU_L34 and the pU_L34 - pU_L31 interaction were required for PKC recruitment to the nuclear rim, the localization of PKC was determined in cells infected with either $vRR1072$, a U_L34 -null virus in which a large portion of the U_L34 open reading frame was deleted (30), or $v3480$, a U_L34 mutant virus lacking a domain (amino acids 138 to 181) essential for interaction with the U_L31 protein (18). In cells infected with either the U_L34 -null virus (Fig. 4J to L) or $v3480$ (Fig. 4M to O), the PKC expression pattern was similar to that seen upon infection with the U_L31 -null mutant. Specifically, a small upregulation of PKC was observed in the cytoplasm of mutant HSV-1-infected cells, but the PKC was not concentrated at the nuclear rim as deduced from the virtual absence of colocalization with lamin B in the nuclear lamina. We conclude that whereas PKC upregulation during HSV-1 infection occurs, at least in part, independently of U_L31 and U_L34 , the recruitment of PKC to the nuclear lamina requires both proteins and also the portion of pU_L34 necessary for pU_L34 - pU_L31 complex formation.

PKC recruitment to the nuclear rim occurs during infection with U_S3 -deficient strains of HSV-1. To investigate the role of the HSV-1 U_S3 protein and its kinase activity in the recruitment of PKC to the nuclear lamina, HEp-2 cells were mock infected or were infected with HSV-1 (F), R7037, a U_S3 -null strain, in which a large portion of the U_S3 open reading frame was deleted, and $vRR1204\#1$ (K220A), a U_S3 kinase-defective strain in which an invariant lysine residue in the catalytic active site at position 220 was mutated to alanine (31). Cells were again fixed at 16 h postinfection, and PKC, lamin B and ICP4 localizations were observed by IFA.

Infection with either U_S3 mutant produced virtually identical PKC localization (Fig. 5G to I and J to L); however, this localization differed from that of PKC in wild-type HSV-1 (F)-infected (Fig. 5D to F) and mock-infected (Fig. 5A to C) cells. In cells infected with the U_S3 mutant strains, PKC was recruited to the nuclear rim and colocalized with lamin B staining of the nuclear lamina. However, unlike cells infected with HSV-1 (F), PKC localization at the nuclear rim of cells infected with either U_S3 mutant resulted in an aberrant localization of PKC. PKC staining at the nuclear rim of cells infected with either U_S3 mutant was unevenly distributed along the rim, with regions of punctate aggregation adjacent to regions of light or discontinuous staining. Ryckman and Roller observed aberrant pU_L34 localization in cells infected with these same mutants (31) which was attributed to vesicular extensions of the NM that line the periphery of the nuclei; it is possible that aberrant localization of PKC at the nuclear rim may also be attributed to these NM vesicles.

HSV-1 infection induces phosphorylation of lamin B and PKC. Models proposing that PKC is recruited to the nuclear lamina to catalyze the phosphorylation of lamin proteins, thereby disrupting the integrity of the lamina, predict a virally induced increase in lamin phosphorylation. Since active PKC is phosphorylated, an increase in PKC phosphorylation should also be detectable in infected cells. To test these possibilities, HEp-2 cells were infected with HSV-1 (F), pulse-labeled with [32 P]orthophosphate, lysed at 16 h postinfection, and immunoprecipitated with antibodies specific for lamin B and PKC. Samples were resolved by SDS-PAGE and processed for autoradiography. As seen in Fig. 6A and D, the phosphorylation states of immunoprecipitated lamin B and PKC were signifi-

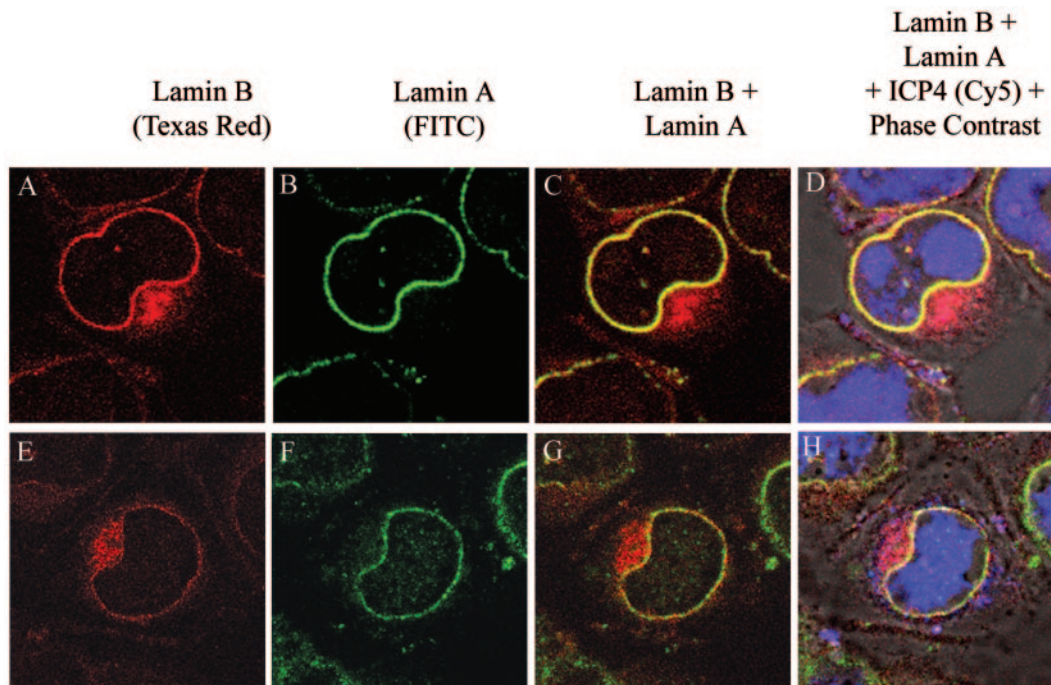


FIG. 7. Digital images of confocal fluorescence micrographs of HSV-1 (F)-infected HeLa cells. At 16 h postinfection, cells were fixed and immunostained for lamin B (Texas Red; red channel), lamin A (FITC; green channel), and ICP4 (Cy5; blue channel).

cantly higher during HSV-1 infection compared to mock infection. Immunoblot assays of replicate crude lysates (Fig. 6B and E) demonstrated that nearly equal amounts of lamin B and PKC were present in the lysates of mock- and HSV-1-infected cells, thus demonstrating that the observed differences in ^{32}P labeling were a consequence of the level of phosphorylation rather than unequal quantities of proteins within the samples. We conclude that the HSV-induced recruitment of PKC to the nuclear rim is accompanied by increased lamin B and PKC phosphorylation.

To more directly test the role of PKC in the HSV-1-induced increase of lamin B phosphorylation, PKC-specific inhibitors were added to infected cultures at 13 h p.i. As shown in Fig. 6C, addition of 10 μM Rottlerin, a PKC inhibitor which preferentially inhibits PKC δ isozymes, resulted in a clear decrease in lamin B phosphorylation compared to untreated infected samples. Addition of 1 μM RO-31-7549, a PKC inhibitor which preferentially inhibits PKC α isozymes, also caused a decrease in lamin B phosphorylation compared to untreated infected samples, although the decrease was less than that of 10 μM Rottlerin-treated cells. Interestingly, despite the reduction in lamin B phosphorylation following treatment with each inhibitor, lamin B phosphorylation was still significantly higher than that of mock-infected cells. This was also the case following treatment with 10 μM bis-imidolylmaleimide I, a broad-spectrum PKC inhibitor (data not shown). This suggests that while PKC contributes to HSV-1-induced lamin B phosphorylation, additional kinases are also likely to be involved.

Differential effects of HSV-1 infection upon lamin B and lamin A. In HSV-1-infected COS cells, the diffusional mobility of LBR has been reported to increase, and both LBR and lamin B have been shown to aggregate in cytoplasmic com-

partments adjacent to morphological alterations in the NM, suggesting their dissociation from the lamina (32). In contrast to lamin B, previous studies have shown that lamin A-C primarily undergoes conformational changes as a result of HSV-1 infection (27). MCMV infection has also been reported to affect lamin B and lamin A-C differently (23).

In order to observe whether lamin A also accumulates in the cytoplasm during HSV-1 infection, we costained HSV-1-infected cells at 16 h p.i. with the same anti-lamin B antibody described above and a chicken polyclonal anti-lamin A antibody (27). The cytoplasmic aggregates of lamin B seen in COS cells are rarely seen in HSV-1-infected HEP-2 cells (data not shown); however, we have frequently observed cytoplasmic lamin B aggregates in HSV-1-infected HeLa cells (Fig. 7A and E), and we therefore chose to observe HeLa cell infection. In infected cells exhibiting robust cytoplasmic lamin B aggregation, we observed very faint (Fig. 7F) or no (Fig. 7B) cytoplasmic lamin A staining. It thus appears that lamin B and lamin A are affected differently by HSV-1 infection.

DISCUSSION

PKC recruitment to the NM and lamin B phosphorylation.

We report here that HSV-1 infection induces a recruitment of PKC α and PKC δ to the nuclear rim of infected cells. This recruitment is accompanied by the phosphorylation of PKC protein, indicating its activation, and an increased level in the phosphorylation state of lamin B proteins. These studies also show that the HSV-1 U_L31 and U_L34 proteins are necessary for PKC recruitment, and the HSV-1 U_S3 kinase is required for proper PKC localization along the nuclear rim. Such observations are potentially significant, because PKCs are be-

lieved to play important roles during apoptotic disassembly of the nuclear lamina. Thus, it is reasonable to hypothesize that the U_L31 and U_L34 proteins recruit PKC to the NM to phosphorylate lamin B and thereby permeabilize the lamina to facilitate access of nucleocapsids to the INM.

In the early stages of apoptosis, PKC α and δ are recruited to the NM (9, 20, 33). Similar phenomena observed in HSV-infected cells suggest that HSV has coopted cellular mechanisms to recruit PKC to the NM. HSV faces an interesting challenge: it must permeabilize the lamina to allow nucleocapsid egress, but it must avoid nuclear membrane destruction inasmuch as an intact lamina is required for transcription and other essential functions (14). Because PKC δ is believed to represent the major lamin kinase that mediates lamina disassembly during apoptosis, whereas PKC α has been shown to have an antiapoptotic function (9), recruitment of both might serve to sufficiently alter the lamina while avoiding more severe effects. A caveat is that while these studies show that lamin B is more highly phosphorylated in HSV-infected cells, and this phosphorylation corresponds to a recruitment of PKC to the nuclear rim, we have not shown that PKC is directly responsible for the observed lamin B phosphorylation. Also, the partial yet incomplete reduction of HSV-1-induced lamin B phosphorylation by PKC-specific inhibitors suggests that additional kinases may be used by HSV-1 to phosphorylate the lamins. Indeed, although PKC recruitment was observed in most of the infected cells, in general PKC staining was relatively light, and there existed a minority of cells, approximately 20% to 30%, in which PKC localization at the nuclear rim was not detected. Therefore, these studies favor the possibility that other viral or cellular lamin kinases (the latter possibility includes mitogen-associated protein kinases and cyclic AMP-dependent protein kinase) also modify lamins in infected cells.

It is unclear how pU_L34, pU_L31, and U_S3 mediate PKC recruitment to the nuclear rim. We have not been able to convincingly demonstrate a direct interaction between PKC and the pU_L34-pU_L31 complex (data not shown), suggesting that their role in recruitment may be indirect. For example, the U_L34 and U_L31 proteins may be involved in recruiting other proteins to form envelopment sites at the inner nuclear membrane, and these might, in turn, play a role in PKC recruitment. It is also possible that the lack of PKC recruitment observed during infection with the U_L34- and U_L31-null mutants is an indirect consequence of the block in viral maturation induced by the loss of U_L34 or U_L31. The role of U_S3 in mediating proper PKC recruitment at the NM is also obscure. It is possible that the aberrant punctate staining of PKC in cells infected with the U_S3 mutant virus is attributable to abnormal vesicular extensions of the NM that line the interior periphery of the nuclei reported in earlier studies of these U_S3 mutant viruses. The well-documented role of US3 as an antiapoptotic factor during viral infection (1, 2) further complicates interpretation of the results by raising the possibility that the aberrant PKC recruitment to the nuclear rim observed during infection with U_S3 mutant viruses may be the result of apoptotic mechanisms separate and distinct from those induced by viral infection. In any case, additional studies are required to elucidate the mechanism and significance of HSV-1-induced PKC recruitment to the NM and the roles of U_L34, U_L31, and U_S3 in this process.

Comparison across herpesvirus families. Mechanisms by which herpesviruses traverse the nuclear membrane may share similarities across herpesvirus subfamilies. Specifically, PKC is also recruited to the NM in cells infected with MCMV (a betaherpesvirus), and this recruitment is dependent on the homologs of U_L31 and U_L34 (M53 and M50, respectively) (23). Moreover, homologs of HSV-1 U_L34 and U_L31 in HSV-2, pseudorabies virus, and more recently Epstein-Barr virus, a gammaherpesvirus (12, 13, 21) also associate, localize at the nuclear membrane, and interact with lamins, further suggesting that these proteins share common functions. It should be noted, however, that differences will no doubt emerge upon more extensive investigation. For example, MCMV recruits conventional PKCs to the NM, whereas the nuclear rim of HSV-1-infected cells contains both PKC α (a conventional PKC) and PKC δ (a novel PKC). Mutagenesis studies also indicate that although the homologous proteins of MCMV and HSV interact with their respective counterparts, the sites of interaction between these proteins differ (5, 18). For example, sequences in MCMV M50 that have no homology to regions of U_L34 are essential for interaction with MCMV M53.

Differential effects on lamins A versus B in HSV-infected cells. Although both A-type and B-type lamins are stable components of the lamina, the *in vivo* organizational relationship between the two lamin types, and specifically whether filaments contain both A- and B-type lamins, is uncertain (14, 22). The two lamin types appear to be affected differently during HSV-1 infection. In this study some lamin B was observed in perinuclear cytoplasmic regions of infected cells, and a similar localization of small amounts of lamin B1 and lamin B receptor were noted by Scott and O'Hare (32). In contrast, effects on lamin A/C are more subtle. For example, previous studies from this laboratory showed that U_L34- and U_L31-dependent differences in lamin A/C staining were observed in mock- versus HSV-1-infected cells, but these differences were epitope dependent. Specifically, antibodies directed against the rod or tail domains of lamin A/C failed to recognize some lamin A/C in infected cells, whereas a polyclonal antibody that recognizes multiple domains of lamin A/C stained the lamina of infected and uninfected cells equally well (27). Thus, HSV-1 infection induces epitope masking or conformational changes in lamin A/C, rather than displacement from the nuclear lamina to the cytoplasm, as is the case for lamin B. CMV also affects lamins A and B differently inasmuch as B-type lamins are phosphorylated to a greater degree than is lamin A/C (23). An interesting possibility is that the HSV-1-mediated effects on lamin B may be related to the conformational effects on lamin A. This is supported by the observations that both are affected by the same proteins, specifically pU_L31 and pU_L34.

ACKNOWLEDGMENTS

We thank Jarek Okulicz-Kozaryn for technical assistance and members of the Baines laboratory for interesting discussions.

These studies were supported by grant R01 AI52341 from the National Institutes of Health.

REFERENCES

1. Aubert, M., J. O'Toole, and J. A. Blaho. 1999. Induction and prevention of apoptosis in human HEP-2 cell by herpes simplex virus type 1. *J. Virol.* 73:10359-10370.

2. **Benetti, L., and B. Roizman.** 2004. Herpes simplex virus protein kinase U_S3 activates and functionally overlaps protein kinase A to block apoptosis. *Proc. Natl. Acad. Sci. USA* **101**:9411–9416.
3. **Bjerke, S. L., J. M. Cowan, J. K. Kerr, A. E. Reynolds, J. D. Baines, and R. J. Roller.** 2003. Effects of charged cluster mutations on the function of herpes simplex virus type 1 U_L34 protein. *J. Virol.* **77**:7601–7610.
4. **Brodie, C., and P. M. Blumberg.** 2003. Regulation of cell apoptosis by protein kinase c δ . *Apoptosis* **8**:19–27.
5. **Bubeck, A., M. Wagner, Z. Ruzsics, M. Lotzerich, Iglesias, I. R. Singh, and U. H. Koszinowski.** 2004. Comprehensive mutational analysis of a herpesvirus gene in the viral genome context reveals a region essential for virus replication. *J. Virol.* **78**:8026–8035.
6. **Buendia, B., A. Santa-Maria, and J. C. Courvalin.** 1999. Caspase-dependent proteolysis of integral and peripheral proteins of nuclear membranes and nuclear pore complex proteins during apoptosis. *J. Cell Sci.* **112**:1743–1753.
7. **Chang, Y. E., C. Van Sant, P. W. Krug, A. E. Sears, and B. Roizman.** 1997. The null mutant of the U_L31 gene of herpes simplex virus 1: construction and phenotype in infected cells. *J. Virol.* **71**:8307–8315.
8. **Chiellini, A., J. F. Whitfield, U. Armato, and I. Dal Pra.** 2002. Protein kinase C-beta II is an apoptotic lamin kinase in polyomavirus-transformed, etoposide-treated pyF111 rat fibroblasts. *J. Biol. Chem.* **277**:18827–18839.
9. **Cross, T., G. Griffiths, E. Deacon, R. Sallis, M. Gough, D. Watters, and J. M. Lord.** 2000. PKC- δ is an apoptotic lamin kinase. *Oncogene* **19**:2331–2337.
10. **Eitel, K., H. Staiger, J. Rieger, H. Mischak, H. Brandhorst, M. D. Brendel, R. G. Bretzel, H. U. Haring, and M. Kellerer.** 2003. Protein kinase C δ activation and translocation to the nucleus are required for fatty acid-induced apoptosis of insulin secreting cells. *Diabetes* **52**:991–997.
11. **Ejercito, P. M., E. D. Kieff, and B. Roizman.** 1968. Characterization of herpes simplex virus strains differing in their effects on social behaviour of infected cells. *J. Gen. Virol.* **2**:357–364.
12. **Farina, A., R. Feederle, S. Raffa, R. Gonnella, R. Santarelli, L. Frati, A. Angeloni, M. R. Torrisi, A. Faggioni, and H. J. Delecluse.** 2005. BFRF1 of Epstein-Barr virus is essential for efficient primary viral envelopment and egress. *J. Virol.* **79**:3703–3712.
13. **Gonnella, R., A. Farina, R. Santarelli, S. Raffa, R. Feederle, R. Bei, H. M. Granato, A. Modesti, L. Frati, H. J. Delecluse, M. R. Torrisi, A. Angeloni, and A. Faggioni.** 2005. Characterization and intracellular localization of the Epstein-Barr virus protein BFLF2: interactions with BFRF1 and with the nuclear lamina. *J. Virol.* **79**:3713–3727.
14. **Gruenbaum, Y., A. Margalit, R. D. Goldman, D. K. Shumaker, and K. L. Wilson.** 2005. The nuclear lamina comes of age. *Nat. Rev. Mol. Cell Biol.* **6**:21–31.
15. **Heald, R., and F. McKeon.** 1990. Mutations of phosphorylation sites in lamin A that prevent nuclear lamina disassembly in mitosis. *Cell* **18**:579–589.
16. **Hocevar, B. A., D. J. Burns, and A. P. Fields.** 1993. Identification of protein kinase C (PKC) phosphorylation sites on human lamin B. *J. Biol. Chem.* **268**:7545–7552.
17. **Knipe, D. M., D. Senechek, S. A. Rice, and J. L. Smith.** 1987. Stages in the nuclear association of the herpes simplex virus transcriptional activator protein ICP4. *J. Virol.* **61**:276–284.
18. **Liang, L., and J. D. Baines.** 2005. Identification of an essential domain in the herpes simplex virus 1 U_L34 protein that is necessary and sufficient to interact with U_L31 protein. *J. Virol.* **79**:3797–3806.
19. **Liang, L., M. Tanaka, Y. Kawaguchi, and J. D. Baines.** 2004. Cell lines that support replication of a novel herpes simplex virus 1 U_L31 deletion mutant can properly target U_L34 protein to the nuclear rim in the absence of U_L31. *Virology* **329**:68–76.
20. **Martelli, A. M., R. Bortul, G. Tabellini, I. Faenza, A. Cappellini, R. Bareggi, L. Manoli, and L. Cocco.** 2002. Molecular characterization of protein kinase C- α binding to lamin A. *J. Cell. Biochem.* **86**:320–330.
21. **Mettenleiter, T. C.** 2002. Herpesvirus assembly and egress. *J. Virol.* **76**:1537–1547.
22. **Moir, R. D., M. Yoon, S. Khuon, and R. D. Goldman.** 2000. Nuclear lamins A and B1: different pathways of assembly during nuclear envelope formation in living cells. *J. Cell Biol.* **151**:1155–1168.
23. **Muranyi, W., J. Haas, M. Wagner, G. Krohne, and U. H. Koszinowski.** 2002. Cytomegalovirus recruitment of cellular kinases to dissolve the nuclear lamina. *Science* **297**:854–857.
24. **Parekh, D. B., W. Ziegler, and P. J. Parker.** 2000. Multiple pathways control protein kinase C phosphorylation. *EMBO J.* **19**:496–503.
25. **Parker, P. J., and J. Murray-Rust.** 2004. PKC at a glance. *J. Cell Sci.* **117**:131–132.
26. **Rao, L., D. Perez, and E. White.** 1996. Lamin proteolysis facilitates nuclear events during apoptosis. *J. Cell Biol.* **135**:1441–1455.
27. **Reynolds, A. E., L. Liang, and J. D. Baines.** 2004. Conformational changes in the nuclear lamina induced by herpes simplex virus type 1 require genes U_L31 and U_L34. *J. Virol.* **78**:5564–5575.
28. **Reynolds, A. E., B. J. Ryckman, J. D. Baines, Y. Zhou, L. Liang, and R. J. Roller.** 2001. U_L31 and U_L34 proteins of herpes simplex virus type 1 form a complex that accumulates at the nuclear rim and is required for envelopment of nucleocapsids. *J. Virol.* **75**:8803–8817.
29. **Reynolds, A. E., E. G. Wills, R. J. Roller, B. J. Ryckman, and J. D. Baines.** 2002. Ultrastructural localization of the herpes simplex virus type 1 U_L31, U_L34, and U_S3 proteins suggests specific roles in primary envelopment and egress of nucleocapsids. *J. Virol.* **76**:8939–8952.
30. **Roller, R. J., Y. Zhou, R. Schnetzer, J. Ferguson, and D. DeSalvo.** 2000. Herpes simplex virus type 1 U_L34 gene product is required for viral envelopment. *J. Virol.* **74**:117–129.
31. **Ryckman, B. J., and R. J. Roller.** 2004. Herpes simplex virus type 1 primary envelopment: U_L34 protein modification and the U_S3-U_L34 catalytic relationship. *J. Virol.* **78**:399–412.
32. **Scott, E. S., and P. O'Hare.** 2001. Fate of the inner nuclear membrane protein lamin B receptor and nuclear lamins in herpes simplex virus type 1 infection. *J. Virol.* **75**:8818–8830.
33. **Shimizu, T., C. X. Cao, R. G. Shao, and Y. Pommier.** 1998. Lamin B phosphorylation by protein kinase C α and proteolysis during apoptosis in human leukemia HL60 cells. *J. Biol. Chem.* **273**:8669–8674.
34. **Simpson-Holley, M., J. D. Baines, R. J. Roller, and D. M. Knipe.** 2004. Herpes simplex virus 1 U_L31 and U_L34 gene products promote the late maturation of viral replication compartments to the nuclear periphery. *J. Virol.* **78**:5591–5600.
35. **Stuurman, N., S. Heins, and U. Aebi.** 1998. Nuclear lamins: their structure, assembly, and interactions. *J. Struct. Biol.* **122**:42–66.
36. **Zhitovsky, B., A. Gahm, and S. Orrenius.** 1997. Two different proteases are involved in the proteolysis of lamin during apoptosis. *Biochem. Biophys. Res. Commun.* **233**:96–101.